

Yrast superdeformed band in ^{59}Cu

C. Andreoiu,^{1,2} D. Rudolph,¹ C. E. Svensson,³ A. V. Afanasjev,^{4,5} J. Dobaczewski,⁶ I. Ragnarsson,⁷ C. Baktash,⁸ J. Eberth,⁹ C. Fahlander,¹ D. S. Haslip,¹⁰ D. R. LaFosse,^{11,*} S. D. Paul,^{8,†} D. G. Sarantites,¹¹ H. G. Thomas,⁹ J. C. Waddington,¹⁰ W. Weintraub,¹² J. N. Wilson,^{10,‡} and C.-H. Yu⁸

¹*Department of Physics, Lund University, S-22100 Lund, Sweden*

²*NIPNE-“Horia Hulubei,” RO-76900, Bucharest, Romania*

³*Nuclear Science Division, Lawrence Berkeley National Laboratory, Berkeley, California 94720*

⁴*Physik-Department, Technische Universität München, D-85747 Garching, Germany*

⁵*Laboratory of Radiation Physics, Institute of Solid State Physics, University of Latvia, LV 2169 Salaspils, Latvia*

⁶*Institute of Theoretical Physics, Warsaw University, PL-00681 Warsaw, Poland*

⁷*Department of Mathematical Physics, Lund Institute of Technology, S-22100 Lund, Sweden*

⁸*Physics Division, Oak Ridge National Laboratory, Oak Ridge, Tennessee 37831*

⁹*Institut für Kernphysik, Universität zu Köln, D-50937 Köln, Germany*

¹⁰*Department of Physics and Astronomy, McMaster University, Hamilton, Ontario, Canada L8S 4M1*

¹¹*Chemistry Department, Washington University, St. Louis, Missouri 63130*

¹²*Department of Physics, University of Tennessee, Knoxville, Tennessee 37996*

(Received 23 May 2000; published 27 September 2000)

High-spin states in ^{59}Cu were populated using the fusion-evaporation reactions $^{28}\text{Si}+^{40}\text{Ca}$ at a beam energy of 125 MeV and $^{36}\text{Ar}+^{28}\text{Si}$ at a beam energy of 143 MeV. The Gammasphere array in conjunction with ancillary detector systems allowed for the identification of a superdeformed rotational band in ^{59}Cu , which was firmly linked to low-spin yrast states. Using directional correlations of oriented states, a spin-parity assignment of $I^\pi=25/2^+$ to the band head was possible. The average quadrupole moment of the band is measured to be $Q_t=(2.24\pm 0.40) e b$. The characteristics of the band are compared to neighboring nuclei and predictions of different mean-field theories.

PACS number(s): 21.60.Cs, 21.60.Jz, 23.20.Lv, 27.50.+e

Superdeformation is by now a widespread phenomenon across the nuclidic chart. Recently, superdeformed (SD) rotational bands were discovered in the light mass $A\sim 60$ region. Following the first observation of a SD band in ^{62}Zn [1], highly and/or superdeformed bands have been observed in a number of weakly populated $N=Z$ nuclei, namely ^{56}Ni [2], ^{58}Cu [3], and ^{60}Zn [4], and in the $N=Z+1$ nucleus ^{61}Zn [5]. The SD band in ^{60}Zn represents the $N=Z=30$ “doubly magic” superdeformed core of the mass region [4].

The configurations of these bands have the leading component $f_{7/2}^{-4}\otimes(fp)^4\otimes g_{9/2}^{A-56}$ ($A-56$ is the number of nucleons in excess of ^{56}Ni , fp denotes the $f_{5/2}$, $p_{3/2}$, and $p_{1/2}$ orbits) with respect to the doubly magic ^{56}Ni $N=Z=28$ spherical core. According to comparisons between the experimental dynamic moments of inertia $J^{(2)}$ for several collective bands and theoretical predictions [6], the quadrupole deformation of the bands increases with the number of $g_{9/2}$ particles involved in their configuration. For the $N=Z$ nucleus ^{58}Cu the average quadrupole deformation of the band is $\beta_2\approx 0.37$ [3], while it is $\beta_2\approx 0.47$ for the band in the doubly magic superdeformed $N=Z$ nucleus ^{60}Zn [4].

In $N=Z$ nuclei the neutrons and protons occupy the same orbitals, which offers the possibility to investigate the pairing correlations between them. The SD band in ^{60}Zn reveals a band crossing at low frequencies [4] which may be explained as a simultaneous alignment of two pairs of $g_{9/2}$ protons and neutrons. Thus it may be expected that the proton alignment remains at about the same frequency in the $^{61}_{30}\text{Zn}$ nucleus. However, it has been found to be absent, which may be taken as a sign for the presence of $T=0$ pairing in the ^{60}Zn band [5]. Similarly, the presence or absence of a neutron alignment in ^{59}Cu might shed more light into the question of the role of $T=0$ pair correlations in $N=Z$ nuclei.

Another interesting aspect in the mass $A\sim 60$ region was the first observation of a prompt discrete proton decay of the band in ^{58}Cu into a spherical state in the daughter nucleus ^{57}Ni [3]. A second case was established in the decay-out of a rotational band in ^{56}Ni into the ground state of ^{55}Co [2]. Estimated energy relations between an expected excitation energy of a SD band in ^{59}Cu and potential daughter states in ^{58}Ni [7] makes ^{59}Cu a good candidate to search for this new exotic decay mode.

High-spin states in the residual nucleus ^{59}Cu were populated in two experiments performed at the 88-Inch Cyclotron at Lawrence Berkeley National Laboratory. Experiment 1 used the fusion-evaporation reaction $^{28}\text{Si}+^{40}\text{Ca}$ at a beam energy of 125 MeV. The 0.5 mg/cm² thin self-supporting ^{40}Ca target was enriched to 99.975%. The experimental setup consisted of the Gammasphere array [8], at that time comprising 83 Ge detectors. The array was operated in con-

*Present address: Department of Physics, State University of New York at Stony Brook, Stony Brook, NY 11794.

†Present address: Tata Institute of Fundamental Research, Bombay 400 005, India.

‡Present address: Niels Bohr Institute, DK-2100 Copenhagen, Denmark.

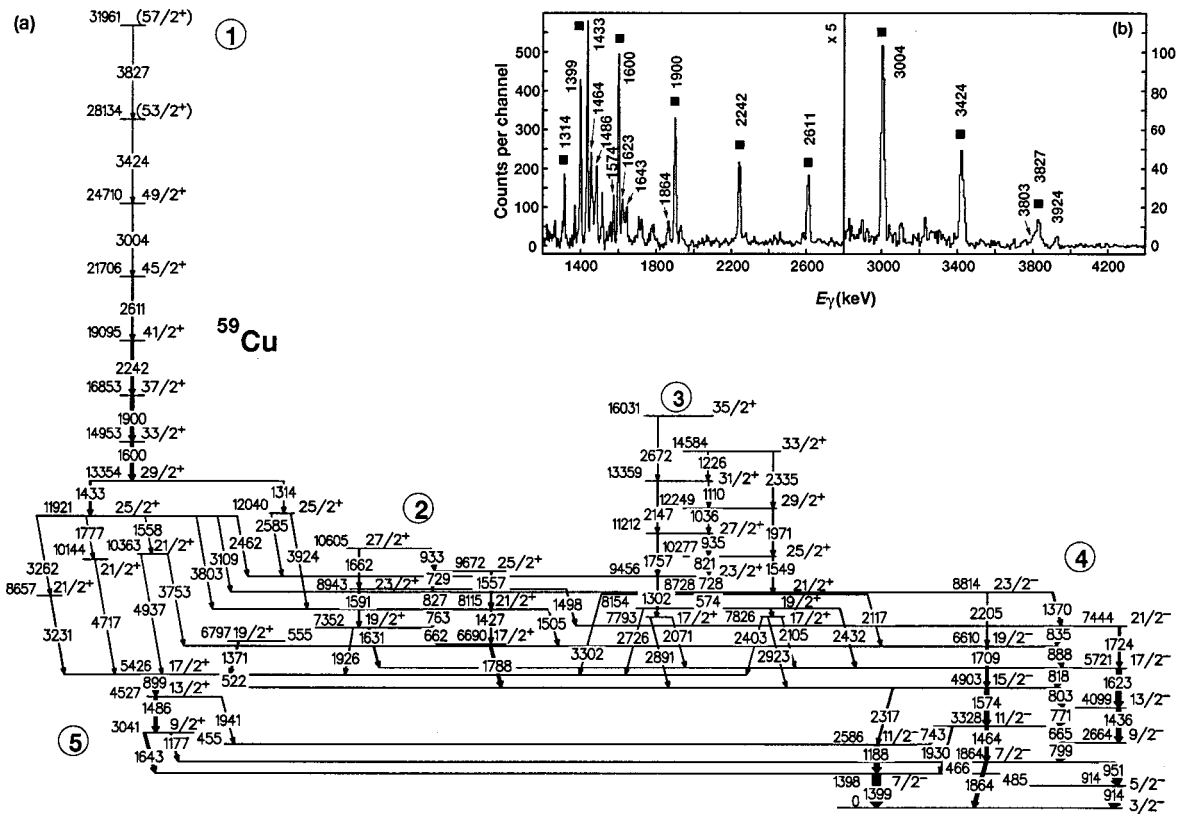


FIG. 1. (a) Proposed partial level scheme of ^{59}Cu . The energy labels are given in keV. The widths of the arrows are proportional to the relative intensities of the γ rays. (b) Gamma-ray spectrum from experiment 2 generated by summing all double gates set on the transitions in band 1. Transitions known to belong to ^{59}Cu [11] and the new transitions from band 1 are labeled with their energies in keV. The latter are also marked with filled squares.

junction with the 4π charged-particle detector array Microball [9] and 15 liquid scintillator neutron detectors. ^{59}Cu represents the $2\alpha 1p$ reaction channel of the reaction providing an experimental relative cross section of $\sigma_{\text{rel}} \approx 5\%$. Experiment 2 used the $^{36}\text{Ar} + ^{28}\text{Si}$ reaction at a beam energy of 143 MeV. The experimental setup was very similar to the one described above, and the details can be found, e.g., in Ref. [10]. Here, ^{59}Cu represents the $1\alpha 1p$ reaction channel with an experimental relative cross section of $\sigma_{\text{rel}} \approx 3\%$. For both experiments, the events were sorted offline into various E_γ projections, E_γ - E_γ matrices, and E_γ - E_γ - E_γ cubes subject to appropriate evaporated particle conditions.

Experiment 1 was the major source for the analysis of ^{59}Cu . The only sizable contamination in the $2\alpha 1p$ -gated spectra originated from the leak through of the $2\alpha 2p$ channel ^{58}Ni ($\sigma_{\text{rel}} \approx 9\%$) when one of the protons escaped detection. We have eliminated this contamination in the analysis by either double γ gating in the cube, or by subtracting identically γ gated spectra obtained from a $2\alpha 2p$ -gated matrix. Experiment 2 provides very high-spin states for ^{59}Cu because there is one less evaporated α -particle to take away excitation energy and angular momentum from the compound system. However, the degree of contamination is much higher because of the leak through of a number of other much stronger channels, e.g., $1\alpha 2p$ ($\sigma_{\text{rel}} \approx 33\%$) or $1\alpha 3p$ ($\sigma_{\text{rel}} \approx 9\%$).

Previously, high-spin states in ^{59}Cu were reported using

the light-ion induced reaction $^{58}\text{Ni}(^3\text{He}, pn)$ at $E_{\text{lab}} = 15\text{--}27$ MeV up to spin and parity $I^\pi = 17/2^-$ at an excitation energy $E_x = 5721$ keV [11]. The main result of our charged-particle gated $\gamma\gamma$ - and $\gamma\gamma\gamma$ -coincidence analysis from the present experiments is the part of the level scheme of ^{59}Cu presented in Fig. 1(a). It focuses on the newly identified superdeformed rotational structure (labeled 1) on the left hand side, which extends the excitation scheme of ^{59}Cu up to $I^\pi = (57/2^+)$ at $E_x = 31.96$ MeV. Band 1 consists of eight intense transitions at 1433, 1600, 1900, 2242, 2611, 3004, 3424, and 3827 keV. The spectrum in Fig. 1(b) is obtained by summing double γ gates set on the band members in the $1\alpha 1p$ -particle gated cube of experiment 2. The last transition at 3827 keV was seen only in experiment 2 for the reasons mentioned above. The band is linked to the low-spin normal deformed yrast states through several weak transitions with typical energies in excess of 3 MeV.

Figure 2 shows two $2\alpha 1p$ -gated γ -ray spectra obtained from experiment 1. The spectrum in Fig. 2(a) is in coincidence with the 1314 keV line, which depopulates the 13 354 keV state in band 1. The peaks at 2585 and 3924 keV link band 1 into the band structures 2 and 3, which subsequently decay mainly into the known [11] negative-parity sequence 4. The spectrum in Fig. 2(b) is in coincidence with the 1433 keV line, which depopulates the same 13 354 keV state in band 1. The peaks at 3262, 3231, 4717, and 4937 keV link band 1 with the known [11] positive-parity states 5. The

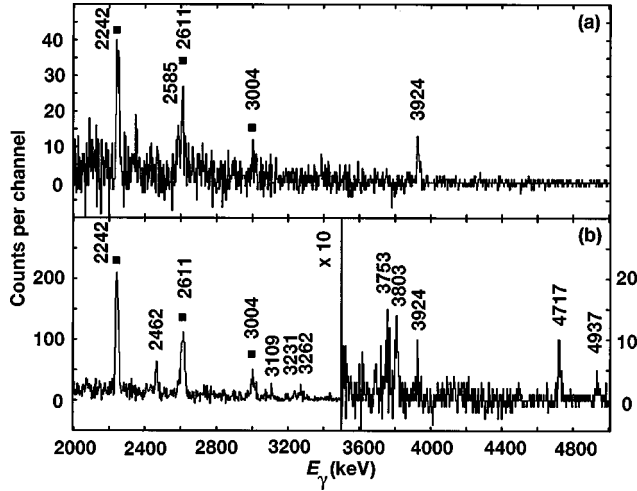


FIG. 2. Two high-energy portions of γ -ray spectra from experiment 1. They are gated by two α particles and one proton detected in Microball. Part (a) is in coincidence with the 1314 keV transition and highlights the two linking transitions at 2585 and 3924 keV. Part (b) is in coincidence with the 1433 keV transition and shows the linking transitions connecting the 11 921 keV $25/2^+$ level in band 1 with states in the first minimum. Squares indicate that the respective transitions belong to band 1.

peaks at 2462, 3109, 3803, and 3753 keV link band 1 also with bands 2 and 3. Here, the 3924 keV line is also present because the 1433 keV line is a doublet with a 1436 keV line which depopulates the 4099 keV $13/2^-$ state in sequence 4.

The linking transitions are very weak relative to the intensity of the in-band transitions of band 1. The intensity of band 1 relative to the 1399 keV ground-state transition is $\approx 30\%$. About half of this intensity is carried by the observed weak linking transitions. Yields of γ rays in coincidence with the 1900 keV transition were used to search for the particle decay-out from band 1. Since the sum of the relative intensities of the ground-state transitions in that spectrum accounts within uncertainties for the intensity of the in-band 1600 keV line, the possibility of prompt proton decay from band 1 is weak. Though searched for, such a decay could not be found in the data sets used in the present analysis.

The assignment of the multipolarities of γ -ray transitions requires the use of directional correlations from oriented states (DCO ratios). For this purpose, we have grouped the Ge detectors in Gammasphere into two “pseudo”-rings labeled 30° (15 detectors at 142.6° , 148.3° , and 162.7°) and 83° (25 detectors at 79.2° , 80.7° , 90.0° , 99.3° , and 100.8°) [10]. A $2\alpha 1p$ -gated γ - γ matrix with γ rays detected at 30° sorted on one axis and 83° on the other axis was created. From this matrix DCO-ratios R_{DCO} were extracted [12]

$$R_{\text{DCO}}(30-83) = \frac{I(\gamma_1 \text{ at } 30^\circ; \text{ gated with } \gamma_2 \text{ at } 83^\circ)}{I(\gamma_1 \text{ at } 83^\circ; \text{ gated with } \gamma_2 \text{ at } 30^\circ)}. \quad (1)$$

Known stretched $E2$ transitions were used for gating. For observed stretched $\Delta I=2$ transitions $R_{\text{DCO}}=1.0$ is expected, while pure stretched $\Delta I=1$ transitions reveal $R_{\text{DCO}}\sim 0.6$.

TABLE I. Gamma-ray energies E_γ and R_{DCO} ratios for band 1 and linking transitions in ^{59}Cu .

E_γ (keV)	R_{DCO}	E_γ (keV)	R_{DCO}	E_γ (keV)	R_{DCO}
1314	1.03(10)	1900	1.01(6)	2923	0.65(21)
1427	1.38(37)	2242	0.93(6)	3004	1.02(10)
1433	0.95(5)	2585	0.26(5)	3231	1.13(17)
1600	1.04(6)	2611	1.16(8)	3262	0.96(20)
1788	0.53(7)	2891	0.42(13)	4717	0.92(27)

Deviations for the latter may arise from quadrupole admixtures, i.e., nonzero $\delta(E2/M1)$ mixing ratios ($M2$ admixtures into $E1$ dipoles are not likely). The results for relevant transitions are summarized in Table I. The DCO ratios for transitions in band 1 are consistent with stretched quadrupole character. To establish the spin and the parity of the 13 354 keV state in band 1, several decay paths of that state can be followed into states with known spin and parity [11].

The last known positive-parity $I^\pi=17/2^+$ state in band 5 at 5426 keV is connected with band 1 via, e.g., the 3231 and 3262 keV lines. The DCO ratios for these two transitions are consistent with stretched $E2$ character, suggesting a $25/2^+$ assignment to the 11 921 keV state. The DCO ratio of the 1433 keV in-band line indicates $E2$ character. This suggests spin and parity $29/2^+$ for the 13 354 keV state. The spins $21/2$ of the 8115 keV state in band 2 and the 8728 keV state in band 3 can be inferred from DCO ratios in Table I and the apparent “coupled-band” structures, i.e., strong $\Delta I=1$ transitions along with parallel quadrupoles. The DCO ratios of the 1788, 2891, and 2923 keV lines connecting bands 2 and 3 with sequence 4 are consistent with pure stretched $\Delta I=1$ character. Because of their relatively high energy this hints towards an $E1$ rather than $M1$ assignment, since for the latter a significant $E2$ admixture can be expected. Moreover, the 8728 keV state in band 3 is connected to the known 5426 keV $17/2^+$ state in band 5 with a single γ ray of 3302 keV. This and more evidence from other combinations leads to a positive-parity assignment to bands 2 and 3. The multipole character of the 2585 keV line, which connects the 12 040 keV state in band 1 with the 9456 keV $23/2^+$ state in band 3, is clearly of mixed $E2/M1$ type (see Table I). Therefore, the spin and parity of the level at 12 040 keV is $25/2^+$ and thus confirms the previous $29/2^+$ assignment to the 13 354 keV state, since the 1314 keV line is also of $E2$ character. It should finally be noted that the large number of observed linking connections and interleaving transitions in the level scheme puts further constraints to the spin and parity assignments.

The experimental dynamic moments of inertia $J^{(2)}$ for the bands in ^{58}Cu [3], ^{59}Cu , ^{60}Zn [1], and ^{61}Zn [5] are compared in Fig. 3(a). The splitting of $J^{(2)}$ at low spin in ^{59}Cu corresponds to the two branches of the SD band via the 1314 keV and 1433 keV transitions. At a rotational frequency of $\hbar\omega\approx 1.0$ MeV an irregularity is present in the ^{60}Zn band, which can be explained in terms of a band crossing due to the simultaneous alignment of pairs of $g_{9/2}$ neutrons and protons. However, the expected proton alignment in ^{61}Zn and

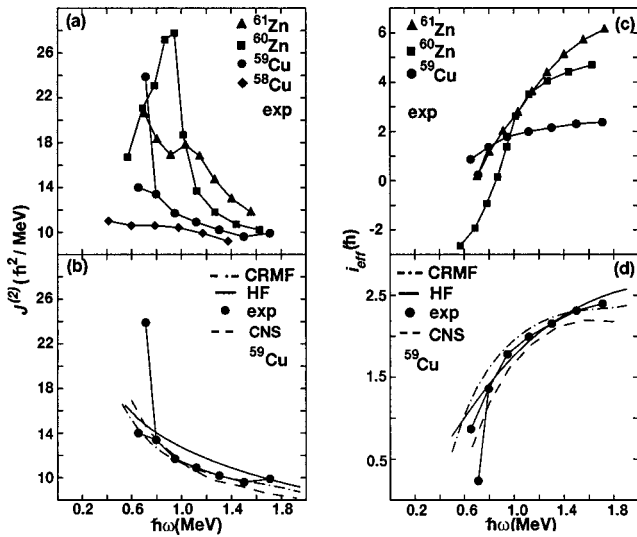


FIG. 3. Part (a) shows the experimental dynamic moments of inertia for the bands in ^{58}Cu , ^{59}Cu , ^{60}Zn , and ^{61}Zn , and part (b) compares the band in ^{59}Cu to several theoretical predictions. Correspondingly, parts (c) and (d) illustrate the effective alignments relative to the band in ^{58}Cu .

the neutron alignment in $^{59}\text{Cu}_{30}$, are not observed at this frequency. The 1433 keV branch of the band in ^{59}Cu leads to the steep increase of $J^{(2)}$ in Figs. 3(a) and (b), which may indicate a band crossing at $\hbar\omega \approx 0.6$ MeV. Hence, the expected alignments in the odd- A neighbors of ^{60}Zn are either absent, or they occur at considerably lower frequencies. Such a delay of band crossing frequency in an even-even nucleus can be a sign of additional neutron-proton correlations [13,14].

Another possible explanation is a change in deformation, the importance of which can be illustrated by an example from $A \approx 150$ region. The yrast SD band in the even-even nucleus ^{150}Gd shows two irregularities, which have been explained in terms of consecutive neutron and proton alignments [15]. In the yrast SD band of the odd- A neighbor ^{151}Tb the paired proton band crossing is blocked by an additional proton in the $i_{13/2}$ orbit, but experiment reveals that the neutron band crossing is substantially quenched as well. This suggests that at superdeformation the properties of the paired band crossing strongly depend both on the configuration and deformation [16]. In a simple picture, however, the smooth increase of deformation when going from ^{59}Cu via ^{60}Zn (see below) towards ^{61}Zn [5] would reveal a band crossing in at least one of the odd- A nuclei, if deformation were the only factor influencing the crossing frequency.

Theoretical calculations for ^{59}Cu have been performed with the cranked relativistic mean-field (CRMF) theory [16] using the NL3 interaction [17], the configuration-dependent cranked Nilsson-Strutinsky (CNS) approach [6], and the cranked Hartree-Fock (HF) method [18] based on the SLy4 force [19]. None of these calculations include pairing, and thus are realistic only at relatively high spins. They all indicate that the configuration $\nu 4^2 \pi 4^1$ ([21,22] in the notation of Ref. [6]) is yrast in the spin range of interest.

In Fig. 3(b), the experimental $J^{(2)}$ of the SD band ^{59}Cu is

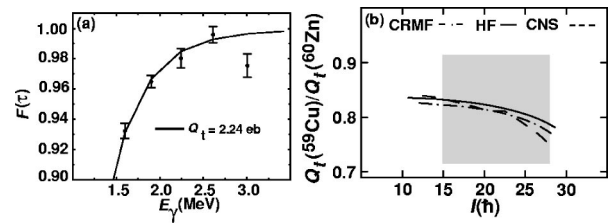


FIG. 4. (a) Fractional Doppler shifts measured for band 1 as a function of γ -ray energy. (b) Ratio of predicted transitional quadrupole moments of ^{59}Cu and ^{60}Zn versus angular momentum. The grey square marks the ratio of the measured average transitional quadrupole moments.

compared with the predictions of the different models for this configuration. They are in excellent agreement with experimental values. The general decrease of $J^{(2)}$ towards high spin can probably be related to the limited angular momentum content of the underlying single-particle configuration [6]. The band in ^{59}Cu approaches the maximum spin value $I_{\text{max}} = 65/2\hbar$, which can be created from the seven valence particles and four holes. At $\hbar\omega = 0.8$ MeV, the calculated angular momenta equal 17.2 (HF), 16.7 (CRMF), and 15.4 \hbar (CNS), and should be compared to the experimental value of 15.5 \hbar . The CNS method gives excellent agreement with data. However, the other two approaches show an excesses of spin which may be required when the standard $T = 1$ pairing correlations are taken into account. These correlations should yield a larger decrease of the calculated spin of ^{59}Cu than that of ^{58}Cu , thus leading to a decrease of the calculated effective alignment.

In Fig. 3(c), the experimental effective alignments i_{eff} of the yrast SD bands in ^{59}Cu , ^{60}Zn , and ^{61}Zn with respect to the ^{58}Cu band are shown. At $\hbar\omega \approx 1.4$ MeV, the magnitude of the alignment for the bands increases nicely with the number of $g_{9/2}$ particles involved in their configurations. The alignment measures the effect of additional particles and the configuration of the band in ^{59}Cu should contain one more neutron in the $g_{9/2}$ orbital than ^{58}Cu , and one proton less than ^{60}Zn . Figure 3(d) compares the effective alignment between the ^{59}Cu and ^{58}Cu bands with the predictions. The fact that all theoretical methods provide an excellent description of the data strongly supports the present interpretation.

Band 1 clearly has all characteristics to represent the yrast SD band in ^{59}Cu . To prove that the transitions belong to such a highly collective structure we employed the fractional Doppler shift method [20]. The measured $F(\tau)$ values for the SD transitions are shown in Fig. 4(a). The average quadrupole moment Q_t of band 1 was determined in exactly the same manner as for ^{60}Zn [4] and ^{62}Zn [1], because the data originates from the same experiment (see Refs. [1,4] for details). Band 1 is best fit by $Q_t = 2.24 \pm 0.40$ e b in the spin range 29/2–49/2 \hbar . The 1433 keV transition was excluded from the simulation due to its doublet structure. For the SD band in ^{60}Zn the value between spin 14 and 28 is $Q_t = 2.75 \pm 0.45$ e b [4]. The errors combine the statistical uncertainties with estimated uncertainties in the stopping powers, while the statistical errors amount to only ± 0.20 e b and ± 0.25 e b for the bands in ^{59}Cu and ^{60}Zn , respectively.

Figure 4(b) shows the ratio of predicted transitional quadrupole moments between ^{59}Cu and ^{60}Zn versus angular momentum. The calculations are performed with the same models as mentioned earlier. The gray square indicates the ratio between experimental average quadrupole moments for ^{59}Cu and ^{60}Zn . This is $R_Q = Q_t(^{59}\text{Cu})/Q_t(^{60}\text{Zn}) = 0.81 \pm 0.10$, determined in the angular momentum interval $I \approx 15\text{--}27 \hbar$. The predicted values for R_Q are lying around ≈ 0.8 , and the experimental uncertainties are clearly too large to allow for a discriminative test of the models.

In conclusion, the level scheme of ^{59}Cu was greatly enlarged, including the identification of the yrast superdeformed band. Linking transitions connecting this band to the low-spin normal deformed yrast states were observed. Using DCO ratios, we have assigned the multipole character to several linking transitions, and subsequently a spin and parity of $I^\pi = 25/2^+$ to the SD band head in ^{59}Cu at 11 921 keV. This is the second case in the mass $A \sim 60$ region for which the spin and parity of the SD band was firmly established. The $J^{(2)}$ moment of inertia and the effective alignment i_{eff} for the ^{59}Cu band were compared to those of bands in neighboring nuclei. Successive patterns suggest a $\nu 4^2 \pi 4^1$ configuration of the SD band in ^{59}Cu . Different theoretical calculations

show an excellent agreement with the experimental values, including absolute and relative quadrupole moments, and thus confirm the configuration assignment. The investigation of ^{59}Cu did not reveal the expected neutron alignment present in ^{60}Zn at $\hbar\omega \approx 1.0$ MeV. Like in the odd-neutron neighbor ^{61}Zn , it is either absent or shifted to lower frequencies. This effect may be attributed to neutron-proton correlations, possibly influenced by the considerable change of deformation, and calls for more detailed theoretical investigations. No prompt proton decay from the SD band in ^{59}Cu was found in the present data sets.

We are thankful for the excellent support at LBNL. This research was supported by the Swedish NSRC, the Polish CSR (KBN No. 2 P03B 040 14), the Canadian NSERC, the German BMBF (06-OK-668), and the U.S. DOE [Grant Nos. DE-FG02-96ER40963 (UT), DE-FG05-88ER40406 (WU), and DE-AC03-76SF0098 (LBNL)]. ORNL is managed by Lockheed Martin Energy Research Corp. for the U.S. DOE under Contract No. DE-AC05-96OR22464. A.V.A. acknowledges support from the Alexander von Humboldt Foundation.

-
- [1] C. E. Svensson *et al.*, Phys. Rev. Lett. **79**, 1233 (1997).
 [2] D. Rudolph *et al.*, Phys. Rev. Lett. **82**, 3763 (1999).
 [3] D. Rudolph *et al.*, Phys. Rev. Lett. **80**, 3018 (1998).
 [4] C. E. Svensson *et al.*, Phys. Rev. Lett. **82**, 3400 (1999).
 [5] C.-H. Yu *et al.*, Phys. Rev. C **60**, 031305 (1999).
 [6] A. V. Afanasjev, I. Ragnarsson, and P. Ring, Phys. Rev. C **59**, 3166 (1999).
 [7] S. M. Vincent *et al.*, Phys. Rev. C **60**, 064308 (1999).
 [8] I.-Y. Lee, Nucl. Phys. **A520**, 641c (1990).
 [9] D. G. Sarantites *et al.*, Nucl. Instrum. Methods Phys. Res. A **381**, 418 (1996).
 [10] D. Rudolph *et al.*, Eur. Phys. J. A **4**, 115 (1999).
 [11] S. Juutinen, J. Hattula, M. Jääskeläinen, A. Virtanen, and T. Lönnroth, Nucl. Phys. **A504**, 205 (1989).
 [12] K. S. Krane, R. M. Steffen, and R. M. Wheeler, At. Data Nucl. Data Tables **11**, 351 (1973).
 [13] D. S. Brenner *et al.*, Phys. Lett. B **243**, 1 (1990).
 [14] S. Frauendorf and J. A. Sheikh, Phys. Rev. C **59**, 1400 (1999).
 [15] W. Nazarewicz, R. Wyss, and A. Johnson, Nucl. Phys. **A503**, 285 (1989).
 [16] A. V. Afanasjev, J. König, and P. Ring, Nucl. Phys. **A608**, 107 (1996).
 [17] G. A. Lalazissis, J. König, and P. Ring, Phys. Rev. C **55**, 540 (1997).
 [18] J. Dobaczewski and J. Dudek, Comput. Phys. Commun. **102**, 166 (1997); **102**, 183 (1997); nucl-th/0003003.
 [19] E. Chabanat, P. Bonche, P. Haensel, J. Meyer, and F. Schaefer, Nucl. Phys. **A635**, 231 (1998).
 [20] B. Cederwall *et al.*, Nucl. Instrum. Methods Phys. Res. A **354**, 591 (1995).